



PAPER • OPEN ACCESS

Biofilm attachment reduction on bioinspired, dynamic, micro-wrinkling surfaces

To cite this article: Alexander K Epstein *et al* 2013 *New J. Phys.* **15** 095018

View the [article online](#) for updates and enhancements.

You may also like

- [3D bioprinting of *E. coli* MG1655 biofilms on human lung epithelial cells for building complex *in vitro* infection models](#)
Samy Aliyazdi, Sarah Frisch, Alberto Hidalgo et al.
- [From molecules to multispecies ecosystems: the roles of structure in bacterial biofilms](#)
Vernita Gordon, Layla Bakhtiari and Kristin Kovach
- [Material properties of biofilms—a review of methods for understanding permeability and mechanics](#)
Nicole Billings, Alona Birjiniuk, Tahoura S Samad et al.

Biofilm attachment reduction on bioinspired, dynamic, micro-wrinkling surfaces

Alexander K Epstein¹, Donggyoon Hong¹, Philseok Kim^{1,2}
and Joanna Aizenberg^{1,2,3,4}

¹ School of Engineering and Applied Sciences, Harvard University,
29 Oxford Street, Cambridge, MA 02138, USA

² Wyss Institute for Biologically Inspired Engineering, 60 Oxford Street,
Cambridge, MA 02138, USA

³ Kavli Institute for Bionano Science and Technology, Harvard University,
29 Oxford Street, Cambridge, MA 02138, USA

E-mail: jaiz@seas.harvard.edu

New Journal of Physics **15** (2013) 095018 (13pp)

Received 22 April 2013

Published 26 September 2013

Online at <http://www.njp.org/>

doi:10.1088/1367-2630/15/9/095018


Abstract. Most bacteria live in multicellular communities known as biofilms that are adherent to surfaces in our environment, from sea beds to plumbing systems. Biofilms are often associated with clinical infections, nosocomial deaths and industrial damage such as bio-corrosion and clogging of pipes. As mature biofilms are extremely challenging to eradicate once formed, prevention is advantageous over treatment. However, conventional surface chemistry strategies are either generally transient, due to chemical masking, or toxic, as in the case of leaching marine antifouling paints. Inspired by the nonfouling skins of echinoderms and other marine organisms, which possess highly dynamic surface structures that mechanically frustrate bio-attachment, we have developed and tested a synthetic platform based on both uniaxial mechanical strain and buckling-induced elastomer microtopography. Bacterial biofilm attachment to the dynamic substrates was studied under an array of parameters, including strain amplitude and timescale ($1\text{--}100\text{ mm s}^{-1}$), surface wrinkle length scale, bacterial species and cell geometry, and growth time. The optimal conditions for achieving up to $\sim 80\%$ *Pseudomonas aeruginosa* biofilm reduction after 24 h growth and $\sim 60\%$

⁴ Author to whom any correspondence should be addressed.



Content from this work may be used under the terms of the [Creative Commons Attribution 3.0 licence](http://creativecommons.org/licenses/by/3.0/). Any further distribution of this work must maintain attribution to the author(s) and the title of the work, journal citation and DOI.

reduction after 48 h were combinatorially elucidated to occur at 20% strain amplitude, a timescale of less than ~ 5 min between strain cycles and a topography length scale corresponding to the cell dimension of $\sim 1 \mu\text{m}$. Divergent effects on the attachment of *P. aeruginosa*, *Staphylococcus aureus* and *Escherichia coli* biofilms showed that the dynamic substrate also provides a new means of species-specific biofilm inhibition, or inversely, selection for a desired type of bacteria, without reliance on any toxic or transient surface chemical treatments.

 Online supplementary data available from stacks.iop.org/NJP/15/095018/mmedia

Contents

1. Introduction	2
2. Results and discussion	4
2.1. Bioinspired dynamic surface design	4
2.2. Combined effects of dynamic strain and micro-wrinkle topography on biofilm attachment	5
3. Conclusion	10
4. Experimental methods	10
4.1. Programmable tensile instrument	10
4.2. Fabrication of periodically wrinkled polydimethylsiloxane elastomer substrates	11
4.3. Bacterial cultures	11
4.4. Biofilm quantification by colony forming units	11
4.5. Imaging	11
Acknowledgments	12
References	12

1. Introduction

Bacteria in their natural state form biofilms—structured, multicellular communities—on surfaces in natural and anthropogenic environments [1, 2]. Biofilms contaminate a wide variety of infrastructure elements, systems and devices, such as plumbing, oil refineries, medical implants and building heating, ventilation and air conditioning networks [3, 4]. Marine fouling, which is precipitated by the accumulation of bacterial biofilm on ship hulls followed by progressively larger marine organisms, increases the fuel expenditure of seafaring vessels by up to 40%. In medical settings, biofilms are the cause of persistent infections—implicated in 80% or more of all microbial cases—releasing harmful toxins, triggering immune response and even obstructing indwelling catheters. Such nosocomial infections affect about 10% of all hospital patients in the United States and result in nearly 100 000 deaths annually [5, 6]. Furthermore, both industrial and clinical contamination are extremely difficult and costly to treat. The cooperative behavior of bacterial cells enables an increased metabolic diversity and efficiency as well as an enhanced resistance to environmental stresses, antimicrobial agents and immune response. For example, some constituent cells enter dormant states invulnerable to many antimicrobials [7–10], and the protein and exopolysaccharide matrix encasing the biofilm physically resists penetration of conventional liquid- and vapor-phase antimicrobials [11].

Clearly, it is advantageous to prevent rather than treat biofilm formation. Indeed, a wide range of bacteria-resistant surfaces have been proposed, but most strategies rely either on a release of biocidal compounds or on inhibiting adhesion [12–15]. In the first case, coatings or bulk materials release agents such as antibiotics, quaternary ammonium salts or silver ions into the surrounding aqueous environment [12]. The second approach has focused on the use of surface chemical functional groups that inhibit protein adsorption as a means to inhibit bacterial adhesion [16, 17]. Current examples include: (i) low-surface-energy, weakly polarizable materials (e.g. Teflon) to minimize van der Waals interactions [17]; (ii) hydrophilic polymeric materials, such as poly(ethylene glycol) (PEG), which form highly hydrated surfaces [18]; (iii) zwitterionic mixed-charge materials [19] or amphiphilic materials [20] that utilize surface inhomogeneities (i.e. charge or hydrophobicity) to resist adhesion of biofilms at the nano- to micrometer scales [21]; or (iv) micro/nanoscale topographical materials to geometrically reduce attachment of biofouling organisms in a narrow length scale range [22].

While some materials are able to transiently resist particular examples of biofouling, none is capable of long-term resistance to bacterial attachment. A fundamental reason is that all of these state-of-the-art anti-biofouling surfaces exist in static forms, i.e. the surface features or chemistry are static or quasi-static in nature. Permanent interactions between such static surfaces and biofilm-forming bacteria can eventually be established depending on the time scales of the adhesion processes. Even if bacteria are unable to attach directly to a substrate, nonspecific adsorption of proteins and surfactants secreted by bacteria to the surface eventually masks the underlying chemical functionality [23–25]. Additionally, any defects or voids in the surface chemistry can serve as nucleation sites for bacterial attachment. Strategies involving leaching of biocides are limited over a longer timescale since their reservoir is finite and subject to depletion [15]. Also, the emergence of antibiotic- and silver-resistant pathogenic strains, along with new environmental restrictions on the use of biocide-releasing marine coatings, has necessitated the development of new strategies [21, 22].

In contrast, the persistent anti-fouling properties of a range of biological surfaces with active, dynamic topographic features have been described. Nature provides some clues to preventing microbial colonization of surfaces by this alternative strategy. For example, while ship hulls constantly amass layers of algae and other microorganisms, materials with topographical features mimicking the skin of sharks have shown increased resistance to marine biofouling at certain length scales [23]. In this case, the shark is in constant motion, and the skin's structures are static. Conversely, the skins of sedentary marine organisms known as echinoderms, e.g., star fish and sea urchins, are densely decorated with spiny, constantly moving microstructures known as pedicellaria that prevent larvae and microorganisms from attaching to the skin [24–26]. Such mechanical frustration of dynamic, physical structures may provide a more persistent and nontoxic form of inhibitive interaction between bacteria and surfaces. Indeed, bacterial cells are already known to respond to surface topography and mechanics, and their behavior can be manipulated using only spatial and mechanical cues [27–29]. Surface attachment is an integral step in biofilm formation that impacts chemical signaling pathways between and within bacterial cells [30]. Dynamic topographical features may influence the arrangement and the resulting behavior of cells on surfaces and affect biofilm development [31]. Yet, the strategy of mechanical frustration—and the role of topographic parameters with respect to surface motion parameters—has not been applied or studied in a synthetic surface as a potential nontoxic solution for controlling bacterial biofilm attachment.

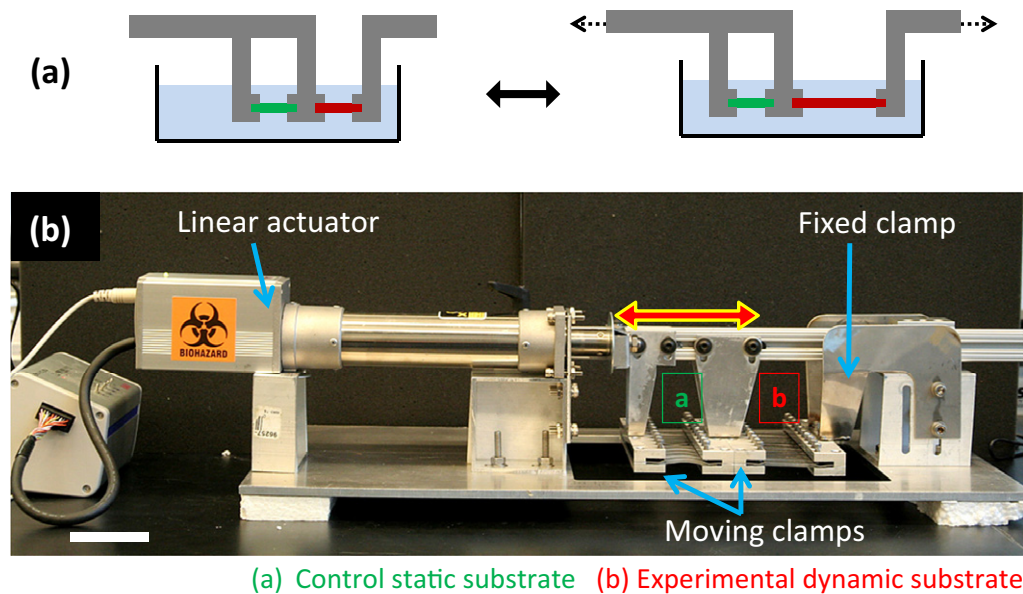


Figure 1. The experimental setup for biofilm growth on dynamic surfaces. (a) Uniaxial strain applied to an elastomeric substrate as a simple bioinspired dynamic surface. (b) A uniaxial tensile instrument was fabricated allowing 20 elastomeric samples to be tested simultaneously. A laptop combined with a logic controller are capable of driving continuous cyclic strain as well as step waveforms (incorporating pauses), and of controlling the strain amplitude and rate. Custom-made grippers independently clamp both static (control) and dynamic substrates submerged in bacterial culture (not shown) during a growth experiment. Scale bar = 5 cm.

Here we report on the development and capability of a synthetic platform inspired by the echinoderm skin to reduce and control bacterial biofilm attachment. The surface in our setup was based on polydimethylsiloxane (PDMS) elastomer with microscale wrinkle topography and on cyclic uniaxial stretching of this surface, which induces sharp transformations of the topography during the extend-release cycle. Bacterial biofilm attachment to the dynamic substrates was studied under an array of parameters, including the mechanical strain amplitude and timescale, surface topography length scale, bacterial species and cell geometry, and growth time. The optimal conditions for achieving up to $\sim 80\%$ *Pseudomonas aeruginosa* biofilm reduction after 24 h and 62% after 48 h were determined through a set of experiments. At the same time, divergent effects on the attachment of *P. aeruginosa*, *Staphylococcus aureus* and *Escherichia coli* biofilm showed that the dynamic substrate also enables an effective new means of species-specific biofilm inhibition—or selection for a desired type of bacteria—without reliance on any toxic or transient surface chemical treatments.

2. Results and discussion

2.1. Bioinspired dynamic surface design

The mechanical frustration strategy of echinoderms' nonfouling skin was adapted in the simplified form of a uniaxially stretching elastic surface, as schematically shown in figure 1(a).

By using an elastomer, the substrate can be cyclically extended and relaxed over time without material degradation. When the substrate is stretched in one direction, it also contracts in the perpendicular directions, due to the Poisson's ratio of an elastomer. Analogous to the moving pedicellaria of the echinoderm, points on the surface of the dynamically strained elastomer move relative to each other during a stretch-release cycle. The biocompatible elastomer PDMS, with an elastic deformation limit of 300%, was chosen for this study [32].

2.1.1. Dynamic strain of target substrate. A custom-made uniaxial tensile instrument was fabricated, allowing 20 elastomeric substrates—10 static and 10 dynamic—to be tested in parallel for attachment of bacterial biofilm. Both continuous cyclic strain as well as arbitrary pauses between strain cycles could be produced by the instrument. The instrument could also be programmed to vary the strain magnitude and rate (i.e. velocity of the grippers). As shown in figure 1(b), the overhead traveling rail carried two sets of movable gripper arrays, in addition to a fixed gripper array attached to the base of the instrument. When clamped in the grippers, the exposed length of each 1×5 cm elastomer substrate was 3 cm, and this length was considered to be 0% strain. To expose substrates to biofilm attachment during experiments, the substrate grippers were submerged in a glass container with bacterial culture.

2.1.2. Elastomer buckle-induced dynamic topography. PDMS treated with oxygen plasma while elastically stretched can generate highly regular and controllable parallel 'wrinkle' topography upon release [33]. This effect is a result of the very thin glass-like layer that forms on the surface of PDMS, which is stiffer than the elastomer and buckles under longitudinal compression when the bulk PDMS is released, as shown in figures 2(a)–(c). For this study, it was found that 60 s of oxygen plasma treatment and a pre-stretch of $\varepsilon = 20\%$ would generate surface micro-wrinkles on the order of $1 \mu\text{m}$ wavelength and aspect ratio ~ 0.5 . Moreover, the wrinkles are oriented transverse to the pre-stretch direction when the substrate is subsequently strained by $\varepsilon < 20\%$; but owing to the perpendicular compression due to the large Poisson's ratio of PDMS, the wrinkles switch to mainly longitudinal orientation for $\varepsilon > 20\%$ [33]. This switching process is reversible and can be performed for $> 100\,000$ times without significant changes in the wrinkle topography. Hence the topography itself is highly dynamic and is mechanically actuated simply by stretching or relaxing the substrate within a narrow strain range about the switching point, as shown in figure 2(d). A minor and inevitable artifact of the fabrication process for dynamic wrinkle topography is the generation of small longitudinal cracks, as seen running perpendicular to the regular wrinkles in figure 2(e). However, these only affect a small fraction of the overall sample surface area.

Since plasma treatment of PDMS leads to vitrification of the surface layer, the surface chemistry is no longer identical to that of native PDMS, but is similar to hydrophilic glass. To ensure identical surface chemistry across all samples in the study, the flat PDMS substrates were also plasma treated but without pre-stretching (figure 2(a)), such that they did not form significant, regular wrinkles.

2.2. Combined effects of dynamic strain and micro-wrinkle topography on biofilm attachment

As imaged by fluorescence microscopy in figure 3(a), the attachment of *P. aeruginosa* PA-14 bacteria on a flat PDMS surface appears random and isotropic, whereas the bacteria spontaneously pattern on static PDMS wrinkles, closely registering with the wrinkle spacing

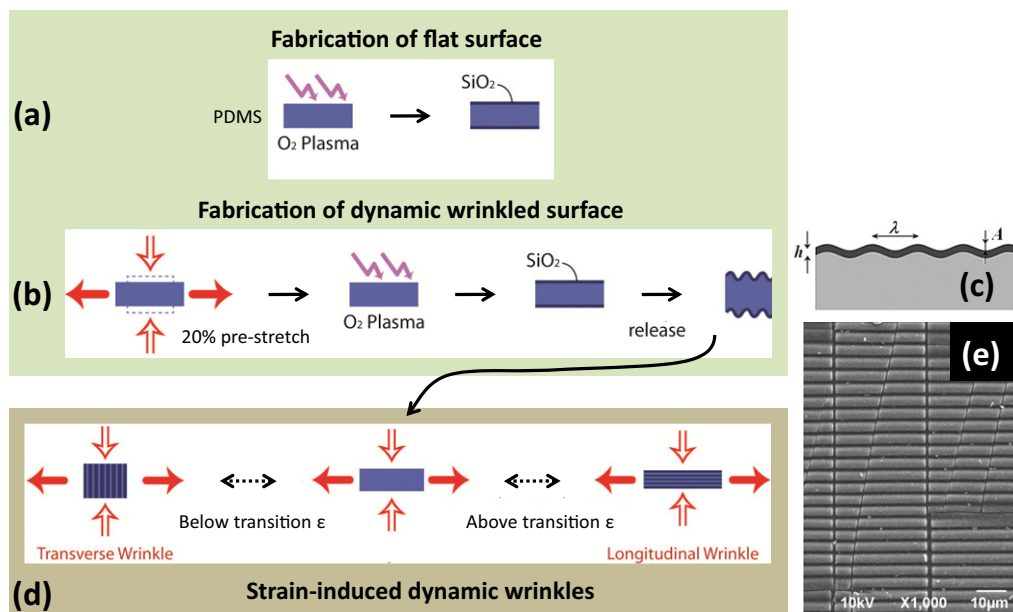


Figure 2. Fabrication and actuation of periodically wrinkled PDMS elastomer substrates. PDMS substrates were treated with oxygen plasma for 60 s to create a nanoscale silica skin, thus presenting identical surface chemistry in all experiments. In contrast to flat substrates (a) that were plasma treated without applied strain, dynamic wrinkle substrates were fabricated by applying a 20% pre-stretch during oxidation. Upon relaxation, highly controlled and regular buckling of the silica skin results, as schematically shown in (c). (d) The pre-stretch amplitude determines a sharp transition point for wrinkle orientation, whereby the wrinkles are transverse below the pre-stretch point and primarily longitudinal above it [33]. (e) SEM image of wrinkled PDMS surface, with regular wrinkles seen in the horizontal direction and small perpendicular cracks, which are a minor fabrication artifact.

and orientation (figure 3(b)). SEM inspection also reveals preferential attachment of bacteria to the troughs of the physical surface features, as seen in figure 3(c). While directed bacterial attachment behavior has also been reported on high aspect ratio pillar arrays [31, 34], the lower aspect ratio structures on the wrinkled PDMS are mechanically more robust and feasible to fabricate on a large scale. We have investigated how introducing dynamic re-orientation of the wrinkles, as well as cyclic tensile strain of the surface, can synergistically frustrate bacterial attachment *a la* marine organisms' active skins.

Combining dynamic strain, dynamic topography and other factors introduced a large parameter space. Potentially relevant parameters were identified as: surface wrinkle length scale; mechanical strain amplitude, time scale and continuous versus intermittent operation; variation of biofilm-forming bacterial species and cell geometry; and bacterial growth time. To probe these effects, a multifactorial design of experiments was conducted.

2.2.1. Uniaxial strain amplitude and time scale. Notwithstanding the 300% elastic limit of PDMS, the practically achievable strain was limited between ~ 5 and $\sim 50\%$ due to the precision

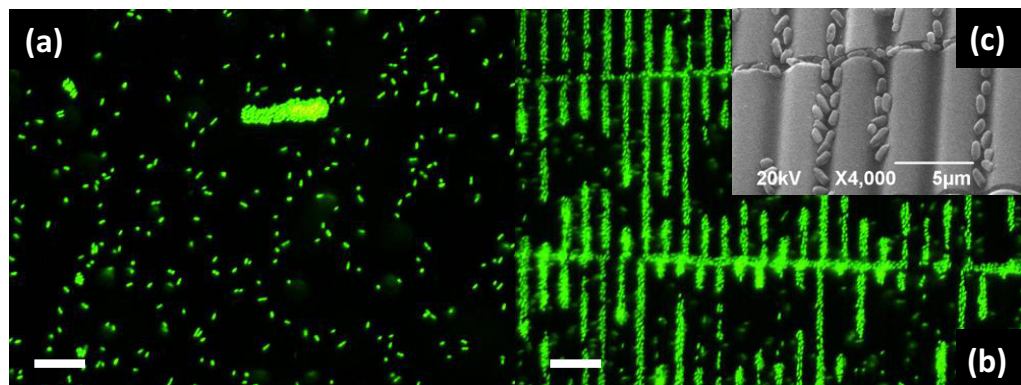


Figure 3. As imaged by fluorescence microscopy, (a) the attachment of *P. aeruginosa* PA-14 bacteria on a flat PDMS surface appears random and isotropic, while (b) the bacteria spontaneously pattern on PDMS wrinkles, reflecting the wrinkle spacing and vertical orientation in the image. The horizontal chains of bacteria follow small perpendicular substrate cracks. (c) SEM image showing the registration of bacteria with the physical surface features. This selective behavior suggests that introducing dynamic re-orientation of the wrinkles as well as tensile strain can frustrate bacterial attachment. Scale bar = 10 μm .

and force limitations of our instrument. Preliminary testing of biofilm attachment following 24 h growth on flat substrates did not show significantly different attachment levels regardless of whether the substrates were cycled between 0% (relaxed) and 10, 0 and 20%, or 0 and 50% strain, suggesting low sensitivity to this parameter. For dynamic wrinkle substrates, a 20% pre-stretch during plasma treatment was adopted. Both small (4%) and large (10%) cyclic strain amplitudes about the 20% pre-stretch point (i.e. 16–24 and 10–30%) were tested for biofilm attachment, also showing no significant difference. Thus strain amplitude larger than 10% (cycling between 10 and 30% absolute strain) was chosen as the standard for all experiments, in light of instrument precision limits and potential for substrates to slightly creep out of the grippers over extended experiments. The fact that large strain magnitudes and/or amplitudes are not critical is a promising factor for the dynamic surface concept's application potential.

P. aeruginosa biofilm was grown for 24 h on flat and wrinkled static substrates, as well as flat and wrinkled dynamic substrates. As seen in figure 4(a), the application of continuous cyclic strain to the flat substrates decreased biofilm attachment by $\sim 56\%$. The addition of wrinkled topography in the static condition increased biomass relative to the flat substrate, consistent with an increase in available surface area for bacteria [31, 34]. However, an attachment decrease of $\sim 78\%$ occurred on dynamic wrinkled substrates versus the static flat substrates—indeed pointing to a synergy of the strain and the dynamic wrinkles that, like the echinoderm skin, serves to frustrate biofilm accumulation.

To minimize energy input and disruption of the anti-fouling surface, the effectiveness of intermittent 'shocks' as opposed to continuous cyclic strain was considered. Dwell times of 5, 18 and 60 min were added between strain cycles, as shown schematically by the inset waveforms in figures 4(b)–(d). However, the introduction of dwell time, particularly beyond 5 min duration, negated the inhibitive properties of dynamic elastomer wrinkles (figures 4(c) and (d)). In these cases, biofilm attachment leveled (or, curiously, even increased) versus a flat

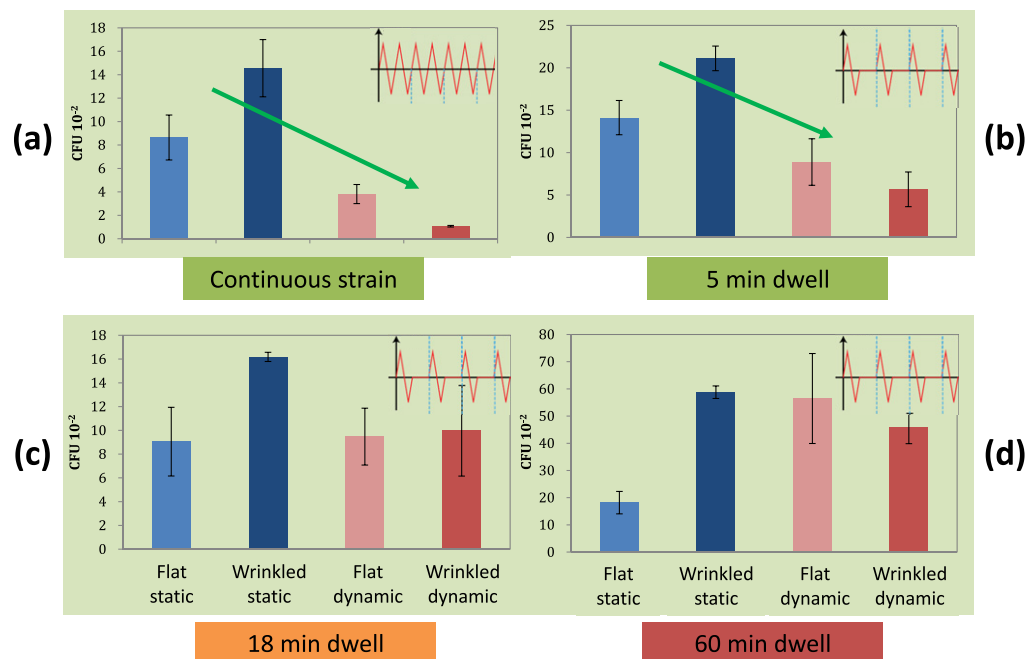


Figure 4. Bacterial biofilm attachment after 24 h growth on elastomeric substrates with respect to topography, dynamic strain (cycling between 10 and 30%), and dwell time between strain events. Insets show schematic waveform of the strain applied to dynamic substrates with respect to time. (a) Continuous strain condition, with no dwell time. (b)–(d) Introduction of dwell time of 5, 18 and 60 min between the strain cycles. Error bars indicate standard deviations.

static substrate. But it is notable that the characteristic viscoelastic relaxation time of a wide range of bacterial biofilms has been reported to be ~ 18 min [35]. As this is the longest time within which a biofilm may mount a phenotypic response to an imposed mechanical force, it stands to reason that dwell times must not be too intermittent in order to still mechanically affect the development of the biofilm.

2.2.2. Topography length scale. Previous work showed that topography on the order of the bacterial length scale would maximize patterned attachment of bacteria [31, 34]. At the same time, studies have suggested that smaller length scale topography can reduce bacterial and other microorganismal attachment due to a geometric decrease in available attachment area [36, 37]. To investigate this point in the context of a dynamic surface, we varied the width of the surface wrinkles by controlling the duration of plasma treatment during substrate fabrication. Submicron wide, ~ 1 or ~ 2 μm wide wrinkle troughs were tested for bacterial accumulation. As shown in figure 5(a), *P. aeruginosa* biofilm attachment decreased $\sim 54\%$ with the addition of submicron wrinkles, but then no further decrease resulted from introducing dynamic strain. It is conceivable that a reduced available surface area also reduces the frustration effects of mechanical strain. Exceeding bacterial dimensions, ~ 2 μm valley width resulted in significantly increased biofilm attachment (figure 5(c)), dominating over inhibition from dynamic strain. Approximately ~ 1 μm valley width appeared to be optimal, yielding the largest attachment decrease of 78% under continuous cyclic strain.

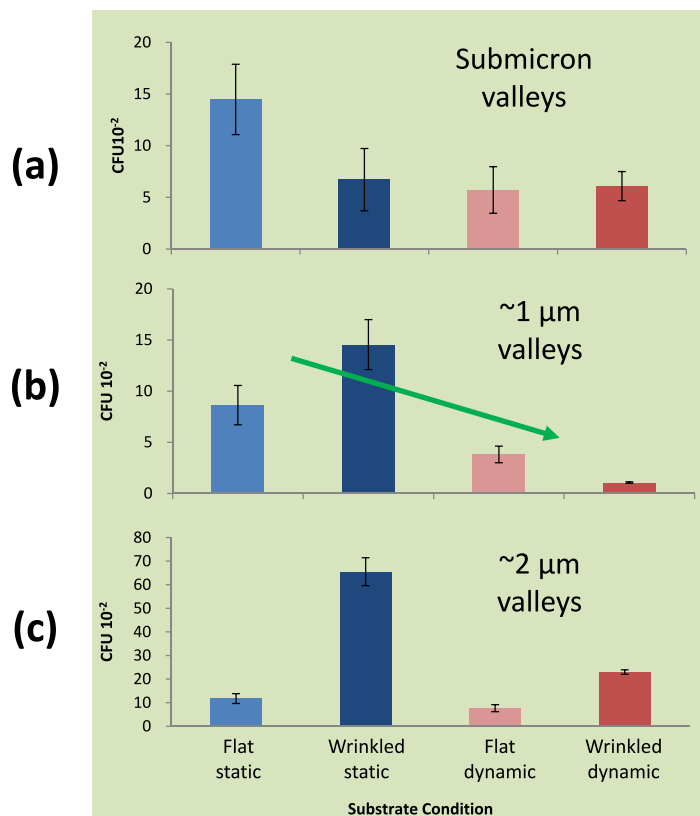


Figure 5. Effect of dynamic elastomer surface wrinkle length scale and continuously applied cyclic strain on 24 h bacterial biofilm attachment. By varying the time of plasma treatment during the substrate fabrication, the width of the surface wrinkles was tuned, and the troughs of the wrinkles were made either (a) submicron wide (10 s plasma treatment), (b) $\sim 1 \mu\text{m}$ wide (60 s treatment), or (c) $\sim 2 \mu\text{m}$ wide (300 s treatment). Error bars indicate standard deviations.

2.2.3. Growth time and bacterial species. Inhibition of *P. aeruginosa* biofilm attachment persisted to 48 h of growth, with 62% reduction in the dynamic wrinkled condition. However, biofilm inhibition at 72 h was more limited, and it resulted only from dynamic strain, not topography, as shown in figure S1 (available from stacks.iop.org/NJP/15/095018/mmedia). The topography no longer provided incremental value over flat static substrates at this extended growth point; in fact, increased growth occurred in the presence of topography in both static and dynamic conditions. Hence, the optimal design of dynamic surfaces for up to 2 days of bacterial exposure may no longer be optimal at 3 days. The factors in this transition remain an open question deserving of future study.

Biofilms in nature are formed by countless different species of bacteria, and they are most commonly comprised of multiple species. In some application contexts, e.g. biomedical devices, a complete lack of biofilm may be desired, while in other cases selectively preventing the adhesion of specific types of bacteria may be advantageous, e.g. on surfaces in the oral cavity [38, 39]. The species dependence of our surface's attachment inhibition was further studied with the biofilm-forming pathogens *S. aureus* MN8 and *E. coli* W3110. As seen in figure S2(a), spherical *S. aureus* bacteria showed no statistically significant attachment relationship

to either dynamic strain or dynamic wrinkle topography, in sharp contrast to *P. aeruginosa* (figure 4(a)). Attachment of *E. coli*, which is rod-shaped like *P. aeruginosa*, actually increased by $\sim 250\%$ in the presence of dynamic strain, yet showed no attachment relationship with respect to topography (figure S2(b)). It is possible that the geometry of the bacterial cell is an important factor in whether a dynamic surface affects biofilm attachment. If so, this raises the intriguing question of why *P. aeruginosa* attachment is inhibited while *E. coli* attachment is promoted under equivalent dynamic and topographic conditions. It may be related to the polar flagellation (attached at ends of cells) of *P. aeruginosa* and the peritrichous flagellation (attached all around cell periphery) of *E. coli*, and thus to the species' different levels of anisotropy and contact modes with the surface [40]. Regardless of the mechanism, our bioinspired synthetic surface platform promises an exceptional new capability for species-specific biofilm inhibition, or inversely, selection for a desired type of bacteria—and without the use of any antibiotics or toxic chemistry.

3. Conclusion

We have demonstrated a novel approach for selectively reducing biofilm attachment—adapting the bioinspired principle of a mechanically frustrating dynamic surface—and potentially obviating the need for biofilm control by toxic release, intensive chemical attack or mechanical removal after the fact. The conditions for achieving up to $\sim 80\%$ *P. aeruginosa* biofilm reduction on biocompatible PDMS after 24 h growth were combinatorially elucidated. From a fabrication standpoint, the dynamically wrinkled surface is extremely simple to produce and scalable to large areas. This method further extends recent attempts to create dynamic surfaces that reduce bacterial attachment due to the organism's inability to establish reliable permanent contacts with the mobile solid or liquid interfaces [41, 42].

Highly divergent effects on the attachment of *P. aeruginosa*, *S. aureus* and *E. coli* biofilm showed that our bioinspired dynamic substrate provides a new means of species-specific biofilm inhibition that does not rely on any toxic or transient surface chemical treatments, or inversely, enables selection for a desired type of bacteria. In future designs, this strategy could be modified to employ smaller strain amplitudes, as the dynamic wrinkle switching does not require more than a few per cent strain difference. It would also be possible to capture passive sources of energy such as wind or ocean waves to drive perpetual cyclic mechanical strain of the surface. For example, an elastomeric buoy tether with dynamic surface wrinkles may continuously extend and relax, driving surface wrinkle switching and the associated attachment inhibition of selected micro-organisms.

4. Experimental methods

4.1. Programmable tensile instrument

A uniaxial tensile instrument was fabricated and assembled, allowing 20 elastomeric samples to be tested simultaneously. A laptop with 'RCPC' control software (IAC) and a programmable logic controller (Moeller easy512 AC-RC) drove an IAC linear servo actuator with 100 N force capacity. Both continuous cyclic strain ($1\text{--}100\text{ mm s}^{-1}$) as well as step waveforms incorporating dwell time could be produced. Metal tab grippers independently clamped the ends of ten static (control) and ten dynamic $1 \times 5\text{ cm}$ substrates, leaving 3 cm of exposed gauge length.

The grippers were submerged in a glass container of bacterial culture during experiments. The container was set atop a magnetic stir plate and a stir bar in the container gently mixed the liquid.

4.2. Fabrication of periodically wrinkled polydimethylsiloxane elastomer substrates

Substrates were cast from Dow Corning Sylgard 184 PDMS, with 10 : 1 base–hardener ratio. The PDMS was mixed, degassed for 1 h, poured to 1 mm thickness in large dishes and cured for 3 h at 70 °C. Uniform PDMS strips of 1 × 5 cm were cut. These were treated on both sides with oxygen plasma for 10, 60 or 300 s to create a nanoscale silica skin, thus presenting identical surface chemistry in all experiments. Flat substrates were plasma treated in the relaxed state, while dynamic wrinkle substrates were fabricated by applying a 20% pre-stretch during plasma treatment. Upon relaxation, highly controlled and regular buckling (wrinkling) of the silica skin resulted. The pre-stretch amplitude determined the transition point for wrinkle orientation, whereby the wrinkles are transverse below the pre-stretch point and primarily longitudinal above.

4.3. Bacterial cultures

Bacterial precultures were prepared by suspending a scraped colony from an agar plate into 10 ml Luria broth in loosely capped tubes and incubating in an orbital shaker (200 rpm, 37 °C) for 18–22 h. *P. aeruginosa* PA-14, *S. aureus* MN8 and *E. coli* W3110 strains were used. For each species, 1% initial seeding concentration of preculture was respectively added to the following biofilm-promoting growth media: tryptic broth (BD Bacto Tryptone), tryptic soy broth supplemented with 0.5% glucose and 3% NaCl, and M9 minimal medium supplemented with 0.2% casamino acids and 0.5% glycerol.

4.4. Biofilm quantification by colony forming units

Following growth experiments, samples were cut off with a scalpel blade while still clamped, resulting in 1 × 3 cm uniform dimensions. The biofilm attachment was quantified by colony forming units as previously reported [34], except that all substrates were bath sonicated in PBS 1 × (Lonza Biowhittaker). In brief, substrates were rinsed twice in deionized water, incubated for 30 min at RT in 15 ml PBS 1 × and bath sonicated for 10 min. Ten-fold serial dilutions were taken, 10 μ l drops of the dilutions were tilt-spread into parallel lines on LB agar plates, and these were incubated 24 h at 37 °C for counting. All conditions were quantified with $n = 5$ samples.

4.5. Imaging

Fluorescence microscopy was performed as described previously [34]. For SEM imaging, samples were fixed for 1 h in 5% glutaraldehyde, serially dehydrated for 1 h in each of 25, 50 and 75% ethanol, followed by overnight in absolute ethanol. Samples were then critical point dried in a Tousimis autosamdri 815B, sputter-coated with ~ 10 nm gold, and imaged on a JEOL JSM-6390LV.

Acknowledgments

We thank Tom Blough for valuable assistance with tensile system upgrade work and integration, Jack Alvarenga for assistance with substrate fabrication development, Ilana Kolodkin for advice and culturing medium and the Professor Losick Lab (Harvard Department of Molecular and Cellular Biology) for use of autoclave facilities. DH was funded by the NSF Research Experience for Undergraduates (REU) program under award no. DMR-0820484. This work was funded in part by the Office of Naval Research under award no. N00014-11-1-0641 and BASF Advanced Research Initiative at Harvard University.

References

- [1] Shapiro J 1998 Thinking about bacterial populations as multicellular organisms *Annu. Rev. Microbiol.* **52** 81–104
- [2] Wilking J N, Angelini T E, Seminara A, Brenner M P and Weitz D A 2011 Biofilms as complex fluids *MRS Bull.* **36** 385–91
- [3] Costerton J, Stewart P and Greenberg E 1999 Bacterial biofilms: a common cause of persistent infections *Science* **284** 1318–22
- [4] Costerton J W and Stewart P S 2001 Battling biofilms—the war is against bacterial colonies that cause some of the most tenacious infections known. The weapon is knowledge of the enemy’s communication system *Sci. Am.* **285** 74–81
- [5] Davies D 2003 Understanding biofilm resistance to antibacterial agents *Nature Rev. Drug Discovery* **2** 114–22
- [6] Klevens R *et al* 2007 Estimating health care-associated infections and deaths in US hospitals, 2002 *Public Health Rep.* **122** 160–6
- [7] Ben-Jacob E, Cohen I and Gutnick D L 1998 Cooperative organization of bacterial colonies: from genotype to morphotype. *Annu. Rev. Microbiol.* **52** 779–806
- [8] Klausen M, Aaes Jørgensen A, Molin S and Tolker Nielsen T 2003 Involvement of bacterial migration in the development of complex multicellular structures in *Pseudomonas aeruginosa* biofilms *Mol. Microbiol.* **50** 61–8
- [9] Stewart P S and Franklin M J 2008 Physiological heterogeneity in biofilms *Nature Rev. Microbiol.* **6** 199–210
- [10] Vlamakis H, Aguilar C, Losick R and Kolter R 2008 Control of cell fate by the formation of an architecturally complex bacterial community *Genes Dev.* **22** 945–53
- [11] Epstein A, Pokroy B, Seminara A and Aizenberg J 2010 Bacterial biofilm shows persistent resistance to liquid wetting and gas penetration *Proc. Natl Acad. Sci. USA* **108** 995–1000
- [12] Banerjee I, Pangule R and Kane R 2010 Antifouling coatings: recent developments in the design of surfaces that prevent fouling by proteins, bacteria, and marine organisms *Adv. Mater.* **23** 690–718
- [13] Genzer J and Efimenko K 2006 Recent developments in superhydrophobic surfaces and their relevance to marine fouling: a review *Biofouling* **22** 339–60
- [14] Meyer B 2003 Approaches to prevention, removal and killing of biofilms *Int. Biodeterioration Biodegradation* **51** 249–53
- [15] Zhao L, Chu P K, Zhang Y and Wu Z 2009 Antibacterial coatings on titanium implants *J. Biomed. Mater. Res. B* **91** 470–80
- [16] Park K D *et al* 1998 Bacterial adhesion on PEG modified polyurethane surfaces *Biomaterials* **19** 851–9
- [17] Prime K L and Whitesides G M 1991 Self-assembled organic monolayers: model systems for studying adsorption of proteins at surfaces *Science* **252** 1164–7
- [18] Bos R, Mei H and Busscher H 1999 Physico chemistry of initial microbial adhesive interactions—its mechanisms and methods for study *FEMS Microbiol. Rev.* **23** 179–230
- [19] Gristina A 1987 Biomaterial-centered infection: microbial adhesion versus tissue integration *Science* **237** 1588–95

- [20] Neu T 1996 Significance of bacterial surface-active compounds in interaction of bacteria with interfaces *Microbiol. Mol. Biol. Rev.* **60** 151–66
- [21] Hall-Stoodley L, Costerton J W and Stoodley P 2004 Bacterial biofilms: from the natural environment to infectious diseases *Nature Rev. Microbiol.* **2** 95–108
- [22] Trevors J 1987 Silver resistance and accumulation in bacteria *Enzyme Microbial Technol.* **9** 331–3
- [23] Schumacher J *et al* 2007 Engineered antifouling microtopographies—effect of feature size, geometry, and roughness on settlement of zoospores of the green alga *Ulva Biofouling* **23** 55–62
- [24] McKenzie J and Grigolava I 1996 The echinoderm surface and its role in preventing microfouling *Biofouling* **10** 261–72
- [25] Campbell A and Rainbow P 1977 The role of pedicellariae in preventing barnacle settlement on the sea-urchin test *Mar. Freshwater Behav. Phys.* **4** 253–60
- [26] Ralston E and Swain G 2009 Bioinspiration—the solution for biofouling control? *Bioinsp. Biomim.* **4** 015007
- [27] Discher D, Janmey P and Wang Y 2005 Tissue cells feel and respond to the stiffness of their substrate *Science* **310** 1139–43
- [28] Huebsch N *et al* 2010 Harnessing traction-mediated manipulation of the cell/matrix interface to control stem-cell fate *Nature Mater.* **9** 518–26
- [29] Stevens M M and George J H 2005 Exploring and engineering the cell surface interface *Science* **310** 1135–8
- [30] Davey M and O'toole G 2000 Microbial biofilms: from ecology to molecular genetics *Microbiol. Mol. Biol. Rev.* **64** 847–67
- [31] Hochbaum A and Aizenberg J 2010 Bacteria pattern spontaneously on periodic nanostructure arrays *Nano Lett.* **10** 3717–21
- [32] Lötters J, Olthuis W, Veltink P and Bergveld P 1997 The mechanical properties of the rubber elastic polymer polydimethylsiloxane for sensor applications *J. Micromech. Microeng.* **7** 145–7
- [33] Kim P *et al* 2013 Rational design of mechano-responsive optical materials by fine tuning the evolution of strain-dependent wrinkling patterns *Adv. Opt. Mater.* **1** 381–8
- [34] Epstein A, Hochbaum A, Kim P and Aizenberg J 2011 Control of bacterial biofilm growth on surfaces by nanostructural mechanics and geometry *Nanotechnology* **22** 494007
- [35] Shaw T, Winston M, Rupp C, Klapper I and Stoodley P 2004 Commonality of elastic relaxation times in biofilms *Phys. Rev. Lett.* **93** 98102
- [36] Boyd R D, Verran J, Jones M and Bhakoo M 2002 Use of the atomic force microscope to determine the effect of substratum surface topography on bacterial adhesion *Langmuir* **18** 2343–6
- [37] Scardino A, Guenther J and De Nys R 2008 Attachment point theory revisited: the fouling response to a microtextured matrix *Biofouling* **24** 45–53
- [38] Gibbons R 1989 Bacterial adhesion to oral tissues: a model for infectious diseases *J. Dental Res.* **68** 750–60
- [39] Orstavik D, Kraus F W and Henshaw L C 1974 *In vitro* attachment of streptococci to the tooth surface *Infection Immunity* **9** 794–800
- [40] Friedlander R S *et al* 2013 Bacterial flagella explore micro-scale hummocks and hollows to increase adhesion *Proc. Natl Acad. Sci. USA* **110** 5624–9
- [41] Epstein A K, Wong T S, Belisle R A, Boggs E M and Aizenberg J 2012 Liquid-infused structured surfaces with exceptional anti-biofouling performance. *Proc. Natl Acad. Sci.* **109** 13182–7
- [42] Li J, Kleintschek T, Rieder A, Cheng Y, Baumbach T, Obst U, Schwartz T and Levkin P A 2013 Hydrophobic liquid-infused porous polymer surfaces for antibacterial applications *ACS Appl. Mater. Interfaces* **5** 6704–11